



Article

Multi-Temporal Analysis of Environmental Carrying Capacity and Coastline Changes in Yueqing City

Zitong Pan ¹, Yi Wang ^{1,*} and Zhice Fang ^{1,2}

¹ School of Geophysics and Geomatics, China University of Geosciences, Wuhan 430074, China; zitongpan@cug.edu.cn (Z.P.); zhicefang@cug.edu.cn (Z.F.)

² Faculty of Geo-Information Science and Earth Observation (ITC), University of Twente, P.O. Box 217, 7500 AE Enschede, The Netherlands

* Correspondence: cug.yi.wang@gmail.com

Abstract: With the rapid development of coastal cities, environmental problems are becoming increasingly severe. Therefore, it is imminent to assess the environmental carrying capacity (ECC) of coastal cities. We take Yueqing City, China, as the study area and establish an ECC evaluation system. For the objectivity and scientificity of this study, the coefficient of variation-back propagation neural network (CV-BPNN) method is used to determine the weight of the indicators and a multi-temporal evaluation is conducted. This paper also explores the relationship between coastline changes and ECC variations for the first time. The results indicate: (1) The ECC of Yueqing City first decreased and then increased, and the inland ECC is better than the coastal area. The future trend is expected to rise. (2) The coastline is continuously extending seaward, and the natural coastline retention rate gradually declines. (3) The coupling coordination degree between the change in the ECC and the change in the coastline shows a trend of “first fluctuation, then stability, and then decline,” and the ecological environment situation was still challenging. (4) Based on the above results, some suggestions are put forward to strengthen coastal ecological development and promote the sustainable development of coastal cities.

Keywords: environmental carrying capacity (ECC); coastline; coastal cities; CV-BPNN; coupling coordination degree



Citation: Pan, Z.; Wang, Y.; Fang, Z. Multi-Temporal Analysis of Environmental Carrying Capacity and Coastline Changes in Yueqing City. *Remote Sens.* **2023**, *15*, 5170. <https://doi.org/10.3390/rs15215170>

Academic Editors: Paul C. Sutton and Guiming Zhang

Received: 4 September 2023

Revised: 12 October 2023

Accepted: 13 October 2023

Published: 30 October 2023



Copyright: © 2023 by the authors. Licensee MDPI, Basel, Switzerland. This article is an open access article distributed under the terms and conditions of the Creative Commons Attribution (CC BY) license (<https://creativecommons.org/licenses/by/4.0/>).

1. Introduction

China's coastal areas make full use of its unique geographical location, convenient transportation, and open policies to communicate with the world and become an important window for China's opening up [1]. In recent decades, the acceleration of urbanization and industrialization in coastal areas has caused the destruction of the ecological environment and seriously affected the coastal ecosystem [2]. The coastal zone is a special zone of ocean–sea–land–air interaction, characterized by complex interface processes, rich natural resources, and a fragile ecological environment [3]. The stability of this region is poor, and once damaged, it will cause a series of environmental problems, bring great pressure to the local environment, even destroy the ecological balance, and limit sustainable development [4]. In order to quantify the impact of human activities on the environment and seek the harmonious coexistence of man and nature, environmental carrying capacity (ECC) has attracted the attention of scholars [5]. ECC has an important impact on social and economic development, and scientific evaluation of ECC has important scientific and practical significance for ensuring sustainable development of coastal areas [6].

ECC refers to the limit of the support capacity of the environment in a certain region for human social and economic activities under a certain environmental state at a certain period, which can quantify the ecological environment level of the study area [7]. Early ECC research primarily obtained evaluation results through subjective weighting methods,

such as expert scoring and the analytic hierarchy process, which affected the objectivity of the assessment [8,9]. After entering the 21st century, with the application of emerging technologies such as geographic information systems and spatial analysis in this field, researchers began to carry out quantitative studies on ECC [10,11]. In order to reduce or eliminate the negative impact of subjective factors on the evaluation results, researchers began to apply objective weighting methods in this field [12], such as principal component analysis, entropy weight, and so on [13–15]. In addition, due to its high precision, strong correlation, and practical value, regional ECC has gradually become a mainstream research direction [16–18].

In the past ten years, the theory and methods of ECC have been further expanded; researchers continuously refine evaluation methods and have proposed the ecological footprint theory [19–21], fuzzy reasoning and driving–pressures–state–impact–response (DPSIR) model [22–24], and a range of valid perspectives and evaluation methods [25–27]. At the same time, ECC methods are increasingly diversified without a fixed research framework [28]. According to the actual situation of the study area, the researchers constructed the local ECC assessment system according to local conditions [29–32]. For example, the construction of the ECC indicator system in inland and coastal areas is different, and the research on ECC in different areas (such as forests and mining areas) also needs to be adjusted accordingly [33,34], which reflects the development of ECC in comprehensive, regional and broad directions [35,36]. In addition, researchers have continuously explored the feasibility of studying ECC in various fields and have made good progress in some of them that have not been involved in ECC, such as water resources, tourism, and resource development, and have gradually become popular [19,37–39]. In addition, In the past five years, the rapid development of geographic information systems has made the spatiotemporal dynamic analysis of ECC gradually become a research hotspot, and researchers have begun to analyze and predict the trend of ECC [40]. According to the long-term ECC of the study area, they select an appropriate model to obtain the development law of ECC and predict the trend in the next few years [41]. At present, the research on ECC presents a trend of integrating long-term monitoring results and multi-factor prediction. Using a time-series assessment method, researchers have shown that the ECC of different regions differs in terms of resource development and utilization intensity, environmental pollution, etc. [42–44]. The ECC model focuses on the complementary relationship between human and natural resources, so it has become one of the important indicators for evaluating regional sustainable development [45,46]. These indicators include but are not limited to aspects such as sustainable resource use, environmental protection, and economic and social development [47]. Therefore, these models have been widely used in the spatiotemporal dynamic analysis of regional ECC.

The research on ECC has achieved good results, but the interaction among natural resources, human activities, and socioeconomic development is extremely complex and affected by cross-scale factors. Therefore, the study of ECC also faces the following challenges:

- (1) The ECC evaluation needs improvement, especially in building differentiated indicators for different regions, and its spatiotemporal analysis capability needs to be enhanced, given its insufficient grasp of future trends.
- (2) The weight of evaluation indicators is affected by subjectivity and uncertainty, and more scientific allocation methods need to be explored.
- (3) ECC evaluation should be combined with other research directions to improve comprehensive analysis and promote urban sustainable development.

In order to deeply solve the above challenges existing in ECC evaluation, this study selects Yueqing City, China, as the study area, selects 18 indicators from four dimensions of environment, society, economy, and pollution, and constructs the ECC evaluation framework. The coefficient of variation–BP neural network (CV-BPNN) is used to increase objectivity and scientificity to assign weights. We conduct an in-depth analysis of ECC's spatiotemporal trends and spatial differences, predict the future ECC, and further explore the relationship between ECC changes and the coastline. This paper is committed to solv-

ing the above problems, and its results have important implications for the sustainable development of coastal cities.

2. Materials and Methods

2.1. Study Area

As shown in Figure 1, Yueqing City is located on the southeast coast of Zhejiang Province, on the north bank of the Oujiang Estuary, connected to Yandang Mountain in the northwest and Haiping Plain in the southeast. The city's land area is 1391 km², and its sea area is 284.3 km². Yueqing Bay is located at 27°5'–28°23' north latitude and 120°57'–121°16' east longitude.

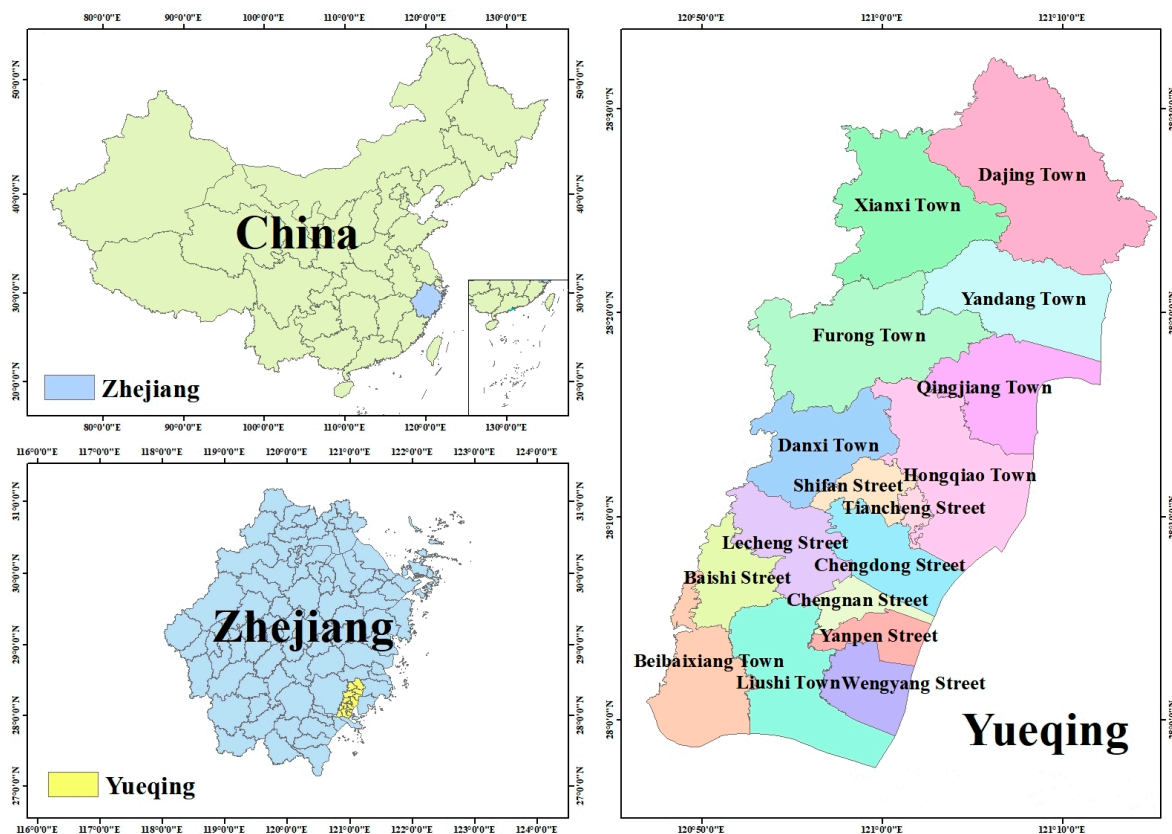


Figure 1. Location of the study area.

The city's administrative area includes 8 subdistricts and 17 towns, with a registered population of 326,511 households and a total population of 111,919. In 2020, Yueqing's GDP reached 126.301 billion yuan, an increase of 4.5% over the previous year, with the primary, secondary, and tertiary industries increasing by 2.2%, 4.3%, and 4.9%, respectively, and the per capita GDP reaching 95,934 yuan (about US\$13,909), up 4.3%. The economic structure of the three major industries was 1.7%, 46.9%, and 51.5%, respectively.

2.2. Available Data

In this paper, taking Yueqing City as the research area, the ECC is analyzed using multi-temporal and multi-spectral remote sensing images. Two remote sensing images are needed to cover Yueqing City. The specific remote sensing data from 2006 to 2020 are listed in Table 1. To ensure the accuracy of subsequent processing, the cloud content of each image is less than 5%. The land use data comes from the 30-m resolution data set released by Wuhan University, rainfall data comes from the Global Rainfall dataset, and the rest of the evaluation indicator data comes from the "Yueqing Yearbook" officially published by the Yueqing Municipal Government.

Table 1. Remote sensing images employed for the study area.

Serial Number	Satellite Sensor	Track Number	Imaging Time	Spatial Resolution
1	Landsat 7 ETM+	118	18 August 2006	30 m
2			18 August 2006	
3			4 June 2008	
4			4 June 2008	
5			25 May 2010	
6			25 May 2010	
7			27 March 2012	
8			27 March 2012	
9	Landsat 8 OLI		13 June 2014	
10			13 June 2014	
11			17 May 2016	
12			17 May 2016	
13	Sentinel-2A	46	22 March 2018	10 m
14			22 March 2018	
15			20 May 2020	
16			20 May 2020	

Before conducting the experiments, it is necessary to preprocess remote sensing images, including radiometric calibration, atmospheric correction, cropping, mosaicking, etc. For statistical data, visualization should be carried out using the ArcGIS 10.7 software.

2.3. ECC Response Mechanism and Technical Route of Coastal Cities

Cities are the main places where human activities are concentrated [48]. From the perspective of urban sustainable development carrying capacity, a city is a complex, comprehensive system coupled with multiple elements, which can generally be divided into environmental, social, and economic subsystems.

Coastal areas tend to be more urbanized and industrialized than inland areas, and the ensuing environmental pollution problems are also more prominent. From the perspective of the sustainable development carrying capacity of coastal cities, pollution is an important issue. Urban pollution will affect the air, water, soil, ecology, and landscape of the city and then affect the sustainable development of the urban environment. In addition, pollution is closely related to the life and health of urban residents. Therefore, pollution can be included in the evaluation system of ECC of coastal cities. The ECC of sustainable development of coastal cities refers to the scale of the population and socioeconomic activities that can be carried by the resource and environmental capacity of a certain regional space to ensure the rational development and utilization of resources and the virtuous cycle of resource development. In the coupling system of environment, society, economy, and pollution (ESEP), the environment is the material basis of social and economic development. The social and economic growth will increase the demand and pressure on the natural environment, and the resulting pollution will have an impact on the environment. The ecological pressure of coastal cities, especially ports and industrial centers, is more obvious. At the same time, as the main body of material production, human beings can improve resource utilization efficiency and pollution control capabilities by increasing investment in the environmental system and the governance of the pollution system. Therefore, the coordinated development of various systems is the key to ECC. The response mechanism of ECC is shown in Figure 2.

According to the basic structure and development characteristics of coastal cities and the response mechanism of ECC, specific evaluation indicators are selected from 4 subsystems, including 18 indicators in terms of positive and negative environments. The specific indicators are shown in Table 2.

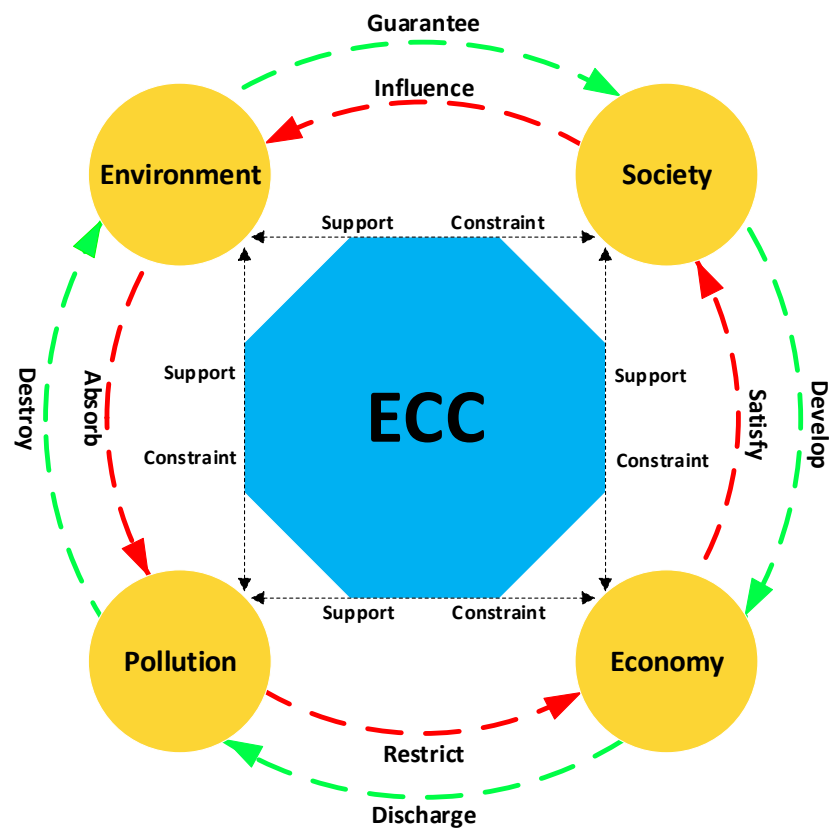


Figure 2. Response mechanism of the ECC for coastal urban system coupled with environment-society-economy-pollution.

Table 2. Comprehensive evaluation indicator system of ECC in Yueqing City.

Target Layer	Subsystem	Indicator Layer	Unit	Indicator Properties
ECC	Environment	Acid rain frequency	-	Negative
		Rainfall	mL	Positive
		NDVI	-	Positive
		Humidity	-	Positive
		Natural coastline retention rate	%	Positive
		Forest coverage	-	Positive
		Population density	-	Negative
		Per capita cultivated area	hm ² /person	Positive
	Society	Industrial electricity consumption	10,000 kW·h	Negative
		Land use index	-	Negative
		Environmental protection investment	Yuan	Positive
		Comprehensive utilization rate of Industrial waste	-	Positive
	Economy	GDP per capita	Yuan	Negative
		Proportion of the tertiary industry	-	Positive
	Pollution	Chemical oxygen demand (COD)	Ton	Negative
		Industrial solid waste discharge	10,000 tons	Negative
SO ₂ emissions		Ton	Negative	
Discharge of wastewater		10,000 tons	Negative	

The entire process of this study is shown in Figure 3.

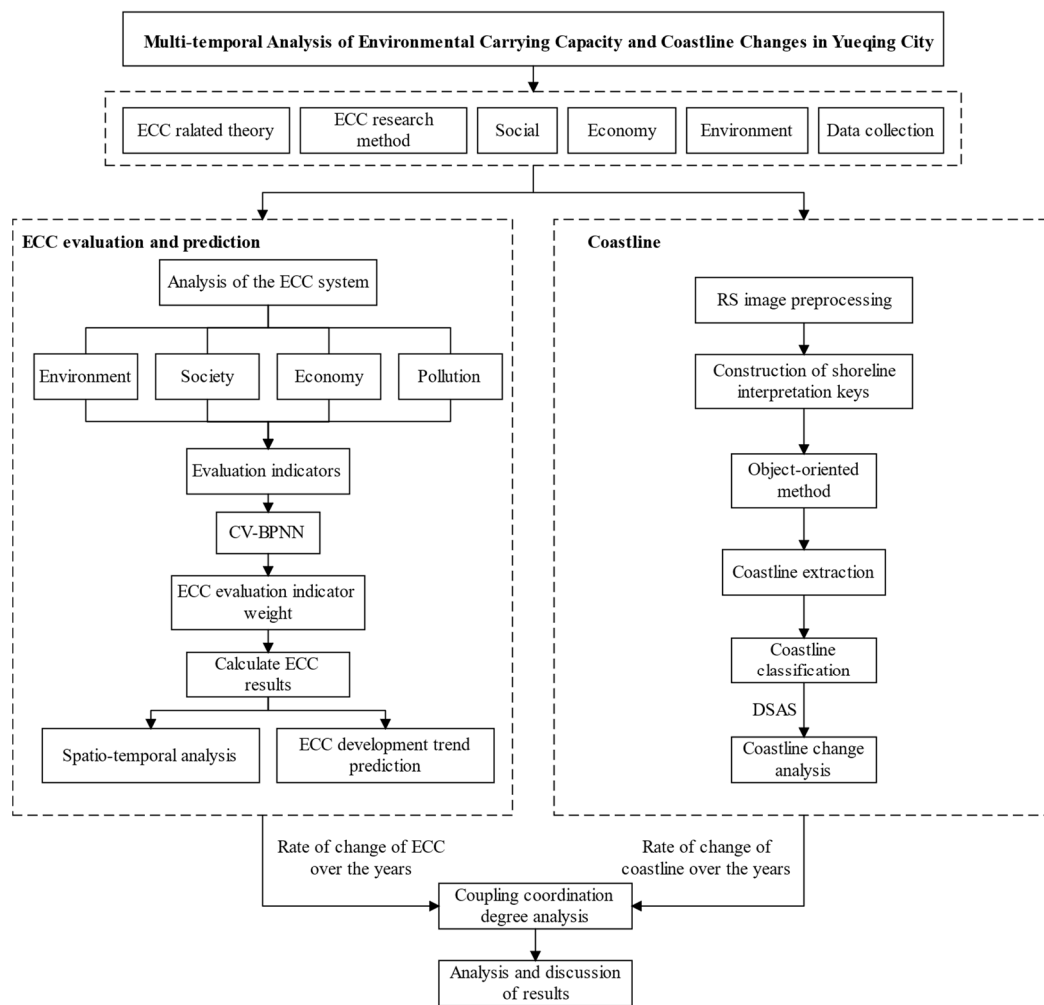


Figure 3. The flowchart of the proposed method.

2.4. ECC Evaluation

2.4.1. Weight Initialization and ECC Calculation

Before assigning weights to each indicator, it is necessary to standardize each indicator due to the differences in their units and magnitudes [49]. Each indicator has either a positive or negative impact on ECC, so the range standardization method is used to process the data. When the indicator is positive, the formula is shown as follows:

$$x = \frac{x_i - \min(x_i)}{\max(x_i) - \min(x_i)} \tag{1}$$

And when the indicator is negative, the formula is shown as follows:

$$x = \frac{\max(x_i) - x_i}{\max(x_i) - \min(x_i)} \tag{2}$$

where x is the initial indicator of the evaluation indicator, x is the standardized value of the evaluation indicator x_i , and $\max(x_i)$ and $\min(x_i)$ are the maximum and minimum values of the indicator, respectively.

After data standardization, initial indicator weights can be calculated. The CV method assigns weights to each indicator based on the individual values and target value variations. If an indicator exhibits significant value disparities, it implies rich discrimination

information, resulting in a higher indicator weight. On the contrary, a smaller weight is assigned to the indicator. The formula is as follows:

$$V_i = \frac{\sigma_i}{\sum_{i=1}^n \bar{x}_i} (i = 1, 2, \dots, n) \quad (3)$$

$$W_i = \frac{V_i}{\sum_{i=1}^n V_i} \quad (4)$$

where V_i is the CV of the i -th indicator, σ_i is the standard deviation of the i -th indicator, \bar{x}_i is the average of the i -th indicator, and W_i is the weight of each indicator.

The ECC of the study area can be calculated using the comprehensive index method of the ArcGIS 10.7 raster calculator as follows [50]:

$$X = \sum_{i=1}^n s_i x_i \quad (5)$$

where X represents the comprehensive score of the ECC, s_i represents the weight of the i -th indicator, x_i represents the standardized value of the i -th indicator data, and n is the number of evaluation indicators.

2.4.2. Weight Optimization

In this study, BPNN is used to optimize index weights. The core concept of BPNN is gradient descent, involving two phases: forward propagation and error backpropagation. In forward propagation, input samples pass through layers, including hidden layers, and reach the output layer. If the output does not match expectations, errors are iteratively sent back, adjusting neuron connections via a weight matrix to minimize errors [51]. After repeated learning, the error is finally minimized.

Applying BPNN requires inputting the numerical values of each evaluation indicator as inputs without the need to construct a fixed model. The initial ECC evaluation results calculated from the initial weights are used as the target output of BPNN. Through extensive learning and training with a large number of samples, the output is compared to the expected value. Training concludes when the error falls below a set threshold, resulting in an adaptive BPNN. Once the ECC evaluation model is obtained, a specific set of sample data is selected for testing [52]. The indicator weights are calculated using the connection weights between neurons [53]. The formula is shown as follows:

$$s_i = \frac{\sum_{l=1}^k |w_{jl}|}{\sum_{i=1}^m \sum_{i=1}^k |w_{il}|}, j = 1, 2, \dots, m \quad (6)$$

where w_{jl} and w_{il} represent the weights from the j -th node to the l -th and from the i -th node to the l -th, respectively, s_i is the optimized weight of evaluation indicator i .

Finally, the ECC is calculated using the optimized weights according to the comprehensive index method.

2.5. ECC Trend Analysis and Prediction

2.5.1. Trend Analysis of ECC

Sen's slope estimator is a median-based approach for long-term series analysis but lacks significance testing for time series trends. In contrast, the Mann–Kendall method is distribution-agnostic and robust to outliers. Combining these methods yields the Sen–Mann–Kendall trend analysis, which incorporates significance testing for time series trends.

The Sen's slope estimator can be calculated as follows:

$$\beta = \text{Median} \left(\frac{x_j - x_i}{j - i} \right), j > i \quad (7)$$

where the trend degree β can judge the rise and fall of the time series trend. When $\beta > 0$, the time series shows an upward trend, and when $\beta < 0$, the time series shows a downward trend.

The Mann–Kendall's formula for time series $X(x_1, x_2, x_3)$ is shown as follows:

$$S = \sum_{i=1}^{n-1} \sum_{j=i+1}^n \text{sgn}(x_j - x_i) \quad (8)$$

where n is the number of sequences, and sgn is the symbol function. When $n < 10$, the statistic is directly used for the bilateral trend test, and when $n > 10$, the statistic roughly obeys the normal distribution, and the test statistic Z is used for the trend test shown as follows:

$$Z = \begin{cases} \frac{S-1}{\sqrt{\text{VAR}(S)}}, & S > 0 \\ 0, & S = 0 \\ \frac{S+1}{\sqrt{\text{VAR}(S)}}, & S < 0 \end{cases} \quad (9)$$

$$\text{VAR}(S) = \frac{n(n-1)(2n+5) - \sum_{i=1}^m t_i(t_i-1)(2t_i+5)}{18} \quad (10)$$

where m is the number of knots (repeated data groups) in the sequence, and t_i is the width of the knot (the number of repeated data in the first repeated data group). In this study, a bilateral trend test is performed on the Z value. At a given significance level α , when $|Z| \geq Z_{1-\alpha/2}$, the trend is significant, and when $|Z| \leq Z_{1-\alpha/2}$, the trend is not significant.

2.5.2. Prediction of ECC

In this study, ECC subsystems are predicted first, and then ECC predicted values are obtained from the predicted values of each subsystem. This study uses MATLAB R2022b for multi-model comparison. It starts by separately fitting subsystem scores to various functions (e.g., polynomial regression, exponential functions, generalized linear models, etc.). The most suitable fitting function for each subsystem is selected based on fitting errors and practical considerations. Next, the relationship between subsystem scores and time is employed to predict future scores. Finally, a comprehensive index method calculates ECC scores for future years using the predicted scores from each subsystem. Hence, the multi-model comparison method offers excellent applicability and flexibility, ensuring accurate and reliable ECC value predictions.

The functions are calculated as follows:

$$y_1 = a_0 + a_1t + a_2t^2 + \dots + a_nt^n + \varepsilon \quad (11)$$

$$y_2 = ae^{bt} + \varepsilon \quad (12)$$

$$g(y) = a + bt + \varepsilon \quad (13)$$

where a , b represent the regression coefficient, ε is the error term, and g is a monotone differentiable connection function, such as a logarithmic function, a logical function, etc.

We assess fitting results and prediction model accuracy using percentage error as follows:

$$\text{Percentage error} = \frac{|y - y_{fit}|}{y} \times 100\% \quad (14)$$

The smaller the percentage error, the higher the accuracy of the prediction model.





2.6. Coastline Analysis

2.6.1. Coastline Extraction

In this study, we use the professional object-oriented classification method to divide the study area into two materials, ocean and others, and then extract their boundaries as

the coastline. Due to the uniform and stable characteristics of the ocean, it is easy to classify, so we directly extracted the ocean, while the remaining land was classified as “others.” The interpretation keys shown in Table 3 are first constructed.

Table 3. Remote sensing interpretation keys for the coastline.

Coastline Type	Interpretation Keys		Characteristics
Natural coastline			Natural coastlines usually refer to objectively existing coastlines that have not been affected by human activities. Its texture is rough and irregular, and its color is usually brown or off-white.
Artificial coastline			Artificial coastlines refer to the coastlines after artificially transforming the natural coastlines. Artificial coastlines usually appear smooth and regular in remote sensing images, and their color is mostly off-white.

Object-oriented classification, based on individual objects rather than pixels, diversifies classification criteria beyond the sole reliance on spectral characteristics in remote sensing images, reducing salt and pepper effects. Hence, this study extracts the study area’s coastline using Trimble eCognition 9.5, a professional object-oriented analysis software [54].

Before classification, remote sensing images need to be segmented. Multi-scale segmentation is employed for image segmentation, considering the spectral factor, smoothness, and compactness of various image bands to group similar pixels into coherent objects. In this study, aiming to extract the coastline between water and land, the modified normalized difference water index (MNDWI) serves as the auxiliary band for image segmentation, effectively distinguishing between water and non-water areas as follows:

$$\text{MNDWI} = \frac{\text{Green} - \text{SWIR}}{\text{Green} + \text{SWIR}} \quad (15)$$

where Green and SWIR represent the green and short-wave infrared bands of remote sensing images, respectively—Figure 4 shows the RGB color composite image and the MNDWI result. The higher the value of the MNDWI, the closer it is to white, and vice versa, the closer it is to black.

In the experiment, the three parameters are adjusted for each image, and the control variable experiment is carried out to obtain the optimal segmentation scale of each image. Then, we classify the segmented images and import the classified images into ArcGIS 10.7 software to extract boundaries, and finally, we obtain the coastline of the study area. Affected by various factors, the classification results in some areas may not be satisfactory, resulting in inaccurate coastline extraction. Therefore, it is necessary to combine the remote

sensing images of the year and Google Earth to correct the coastline in ArcGIS 10.7 to make it more realistic.



Figure 4. RGB image and MNDWI result. (a) RGB color composite image, and (b) MNDWI.

2.6.2. Baseline Method

In this paper, the Digital Shoreline Analysis System (DSAS) is used to analyze coastline changes. The analysis principle is shown in Figure 5.

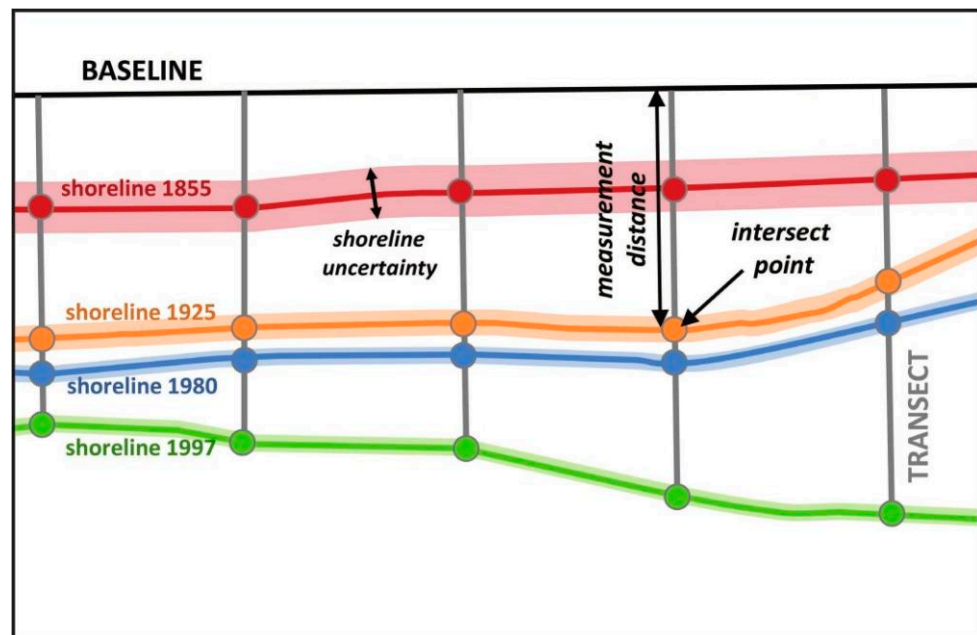


Figure 5. DSAS schematic diagram (<https://www.usgs.gov>, accessed on 9 July 2023).

The end point rate (EPR) is calculated by dividing the distance of coastline position movement in two periods by the time interval. The formula is as follows:

$$EPR_{(i,j)} = \frac{d_j - d_i}{\Delta Y_{(j,i)}} \quad (16)$$

where $EPR_{(i,j)}$ represents the end-point variability between the profile line and the i th and j th shoreline, while d_i and d_j represent the distance from the intersection point of the profile line and the i th and j th shoreline to the baseline, and $\Delta Y_{(j,i)}$ is the time interval between phase i and phase j .

The linear regression rate (LRR) refers to the linear regression fitting of the intersection point between the profile line and the coastline using the least squares method. The slope in the fitting formula is the coastline change rate, and the formula is as follows:

$$y = a + bx \quad (17)$$

$$a = \sum_{i=1}^n (x_i - x)(y_i - y) \quad (18)$$

$$b = y - ax \quad (19)$$

where x represents the year, y represents the spatial position of the coastline, and a represents the fitted constant intercept. And b represents the linear regression rate LRR, which is the change in y for every change in x .

2.7. The Coupling Coordination Degree of ECC Changes and Coastline Changes

In order to better understand the overall coordination effect between subsystems and reflect the degree of coordination, the coupling coordination degree formula is introduced:

$$D = \sqrt{C \times U} \quad (20)$$

where D represents the coupling coordination degree, and the larger D is, the better the coupling coordination degree is. C represents coupling degree $U = \alpha U_a \times \beta U_b$, U_a and U_b represent the subsystem values, respectively, and α and β represent the weights of the two systems.

This paper divides the coupling coordination degree into 10 levels by referring to previous research results, as shown in Table 4.

Table 4. Coupling coordination degree classification.

Coupling Coordination Degree D	Coordination Level
(0.0~0.1)	Extremely dysfunctional
[0.1~0.2)	Severely dysfunctional
[0.2~0.3)	Moderately dysfunctional
[0.3~0.4)	Mildly dysfunctional
[0.4~0.5)	Near dysfunctional
[0.5~0.6)	Barely coordinated
[0.6~0.7)	Primary coordinated
[0.7~0.8)	Intermediate coordinated
[0.8~0.9)	Good coordination
[0.9~1.0)	Quality coordination

3. Results

3.1. ECC Results

3.1.1. Weight Determination

Due to the large amount of selected ECC indicator data, this study randomly selected 8000 pixels at different locations to comprehensively evaluate ECC according to the indicator weight determined by the VC method. After the sample data were collected in the experiment, we selected a three-layer network structure, used MATLAB R2022b software to build a BPNN within the range of hidden layer nodes, and used the sample data of 18 evaluation indicators for learning and training. Then, 5600 samples of the standardized data were randomly selected for training, and the remaining 2400 samples were randomly divided into two as the validation set and test set. After the 5600 data training converged, the overall error of different hidden layer models was compared, and the number of neurons in the hidden layer was finally determined to be 10. After determining the number of hidden layer nodes, we use the training data to train the model using the Levenberg–Marquardt algorithm. Figure 6a shows that the model is trained after 84 iterations and achieves an accuracy of 9.3559×10^{-5} , and Figure 6b demonstrates that the model performs well in predicting the results of training, validation, testing, and overall samples since all R values are over 0.9 and close to 1. After the training of all samples is completed, the connection weights from the input layer to the hidden layer and from the hidden layer to the input layer are obtained, and the optimized weights of each indicator are obtained by Equation (6).

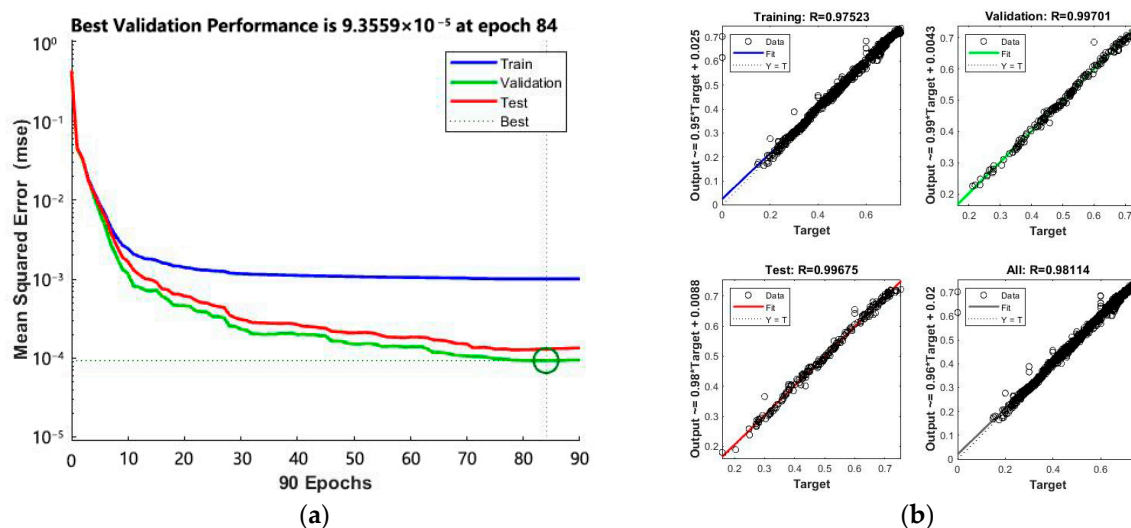


Figure 6. Model training and predictive performance. (a) Training procedure. (b) Predictions of training, validation, testing, and overall samples.

The weights of each indicator before and after optimization are listed in Table 5. It can be observed that the optimization weight is optimized and adjusted for individual indicators whose initial weight is too large or too small to reduce their dependence on data.

Table 5. Weights of each indicator before and after optimization.

Target Layer	Subsystem	Indicator Layer	Initial Weight	Optimizing Weight
ECC	Environment	Acid rain frequency	0.1131	0.0573
		Rainfall	0.0302	0.0428
		NDVI	0.0624	0.0386
		Humidity	0.0057	0.0436
		Natural coastline retention rate	0.0656	0.0583
		Forest coverage	0.0690	0.0523
		Population density	0.0271	0.0460
		Per capita cultivated area	0.0865	0.0673
	Society	Industrial electricity consumption	0.0552	0.0619
		Land use index	0.0433	0.0529
		Environmental protection investment	0.0663	0.0575
		Comprehensive utilization rate of industrial waste	0.0330	0.0578
	Economy	GDP per capita	0.0474	0.0539
		Proportion of the tertiary industry	0.0839	0.0654
	Pollution	Chemical oxygen demand (COD)	0.0706	0.0608
		Industrial solid waste discharge	0.0687	0.0599
SO ₂ emissions		0.0550	0.0586	
Discharge of wastewater		0.0443	0.0650	

3.1.2. Evaluation Results

Figure 7 shows the ECC evaluation results of Yueqing City from 2006 to 2020. The spatial distribution characteristics of ECC have remained similar over the years. Influenced by the terrain, the northwest part of Yueqing City is primarily mountainous, characterized by a good ecological environment, abundant natural resources, lower population density, and limited commercial and agricultural activities, resulting in generally higher scores in ecological environment assessments. Yueqing City’s terrain slopes from northwest to southeast, and the southeastern coastal areas mostly consist of plains adjacent to Yueqing Bay. It is characterized by higher population density and higher economic and development

levels compared to the inland areas. With the rapid development of Yueqing City, this region's ecological environment and natural resources are facing greater pressure, leading to lower ECC scores in the southeastern region.

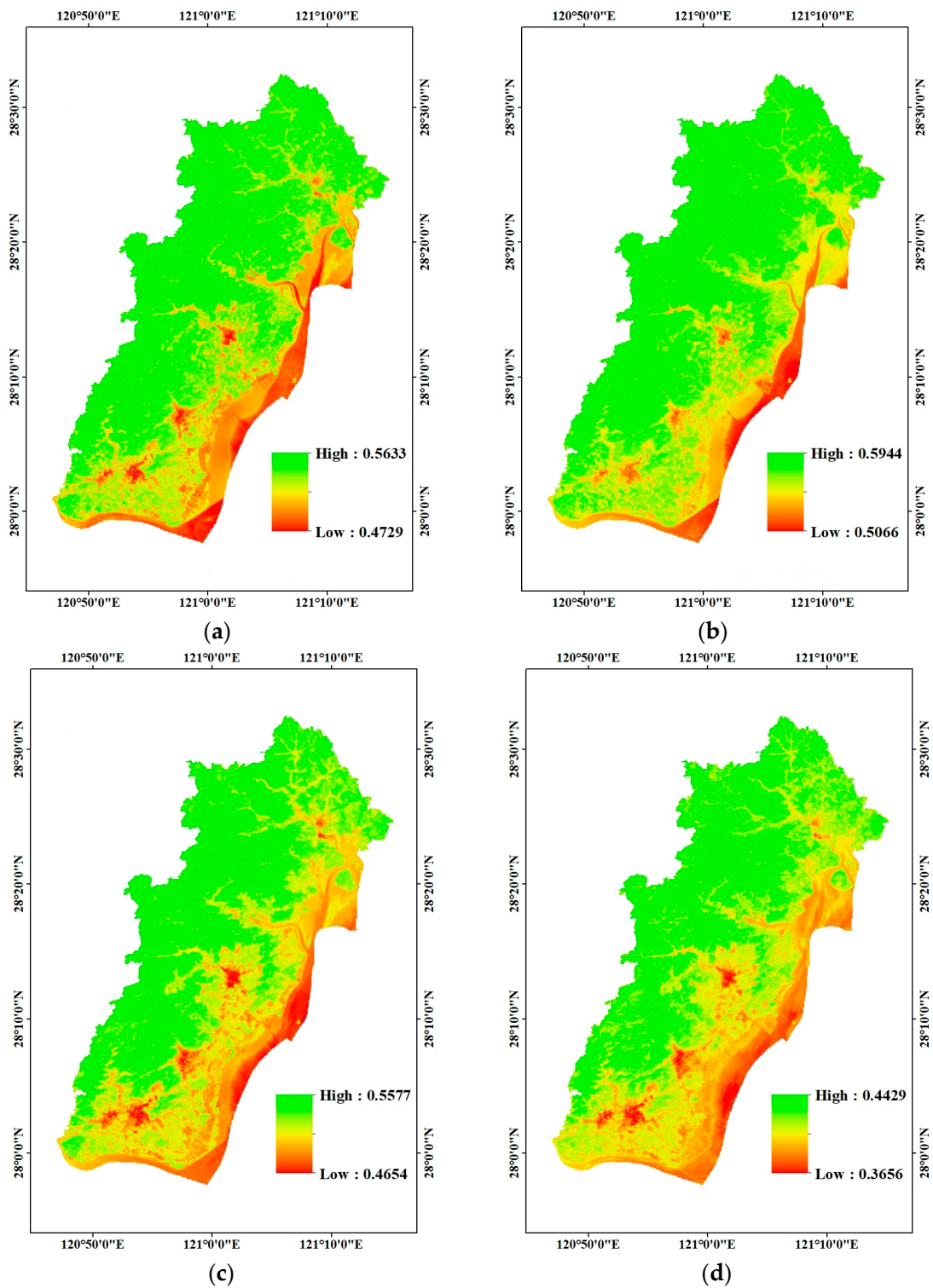


Figure 7. Cont.

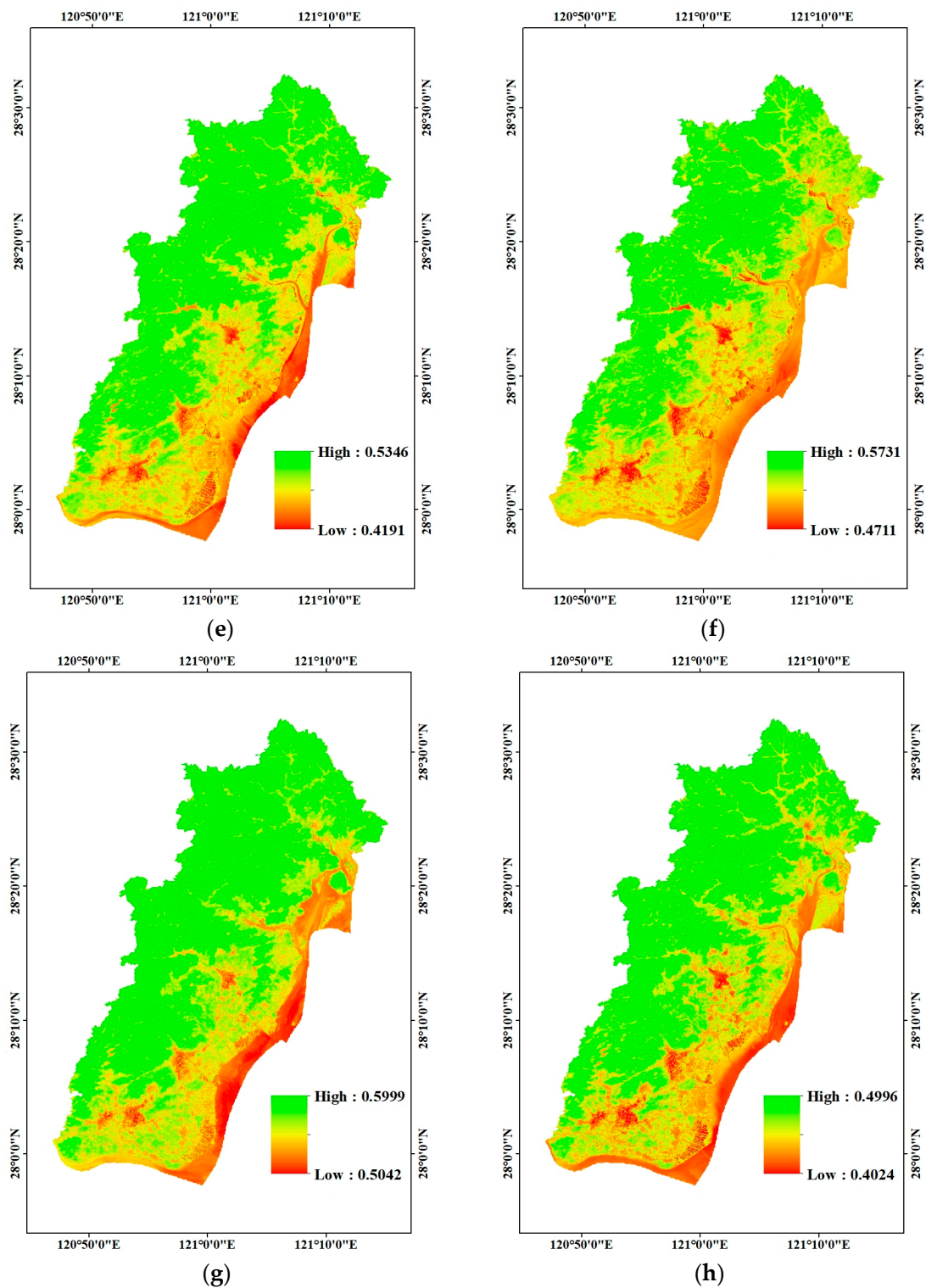


Figure 7. Evaluation results of the ECC in Yueqing City from 2006 to 2020. (a) 2006, (b) 2008, (c) 2010, (d) 2012, (e) 2014, (f) 2016, (g) 2018 and (h) 2020.

In this study, the evaluation results are divided into five grades according to the ECC scores: loadable (0.8, 1], weakly loadable (0.6, 0.8], critical load (0.4, 0.6], overload (0.2, 0.4], and heavy overload (0, 0.2]. Ignoring the grading interval with very few pixels, according to this grade, the ECC grading results of Yueqing City in different years are listed in Table 6. From 2006 to 2020, the ECC of Yueqing City exhibited a downward trend with fluctuations. The decline from 2006 to 2012 can be attributed to imbalanced economic

development during a period of rapid growth driven by urbanization and economic expansion, leading to increased resource consumption and pollution. During the “Twelfth Five-Year Plan” period, Yueqing City focused on ecological protection and the construction of “811” ecological civilization, achieving significant results in improving the ecological environment and reducing pollution. By 2018, ECC had returned to the level seen in 2006. In the “Thirteenth Five-Year Plan” period, increased investments in environmental protection, stricter enforcement of environmental laws, and heightened public awareness led to further improvements in the ecological environment. However, due to the adverse effects of previous rapid development, the ECC still experienced a decline in 2020. In comparison to 2006, this period marked a partial recovery of the environment but remained in an unstable state, underscoring ongoing challenges and contradictions in environmental protection efforts. A significant gap persists between the current environmental quality and public expectations.

Table 6. The grading distribution ratio and average score of the ECC every two years in Yueqing City from 2006 to 2020.

Years	2006	2008	2010	2012	2014	2016	2018	2020
Overload (0.35–0.4)	0	0	0	11.67%	0	0	0	0
Critical load (0.4–0.45)	0	0	0	88.33%	0	0	0	13.24%
Critical load (0.45–0.5)	1.59%	0	2.39%	0	40.58%	0	0	86.76%
Critical load (0.5–0.55)	75.96%	16.15%	94.26%	0	59.42%	60.27%	16.13%	0
Critical load (0.55–0.6)	22.45%	83.85%	3.35%	0	0	39.73%	83.87%	0
Average ECC	0.5739	0.5668	0.5325	0.4179	0.5013	0.5421	0.5717	0.4728

3.1.3. Sen’s Slope Estimator and Mann-Kendall Trend Test

In this section, we superimpose the ECC evaluation results of Yueqing City from 2006 to 2020 and use Sen’s slope estimator and the Mann–Kendall trend test to analyze the ECC’s temporal and spatial change trend and significance in Yueqing City. Figure 8 shows the spatial changes and significant changes in ECC in Yueqing City. It can be seen from Figure 8a that most of the study areas show a slight upward trend, while some areas show a downward trend. Combined with remote sensing images, it can be seen that most of the decline areas are located in the coastal areas. According to the Mann–Kendall significance test results, it can be divided into a slight significant decrease ($-1.96 < S < -0.05$), no significant ($-0.05 < S < 0.05$), and a slight significant increase ($0.05 < S < 1.96$). Figure 8b shows the significance test plot. It can be seen that the ECC in the study area shows a slight upward trend as a whole from 2006 to 2020, and the change is not significant in some areas and the slight downward trend is mainly distributed in the coastal areas.

3.1.4. Prediction of ECC of Yueqing City

In this subsection, the model comparison method is used to fit each subsystem and to find the most suitable fitting function for each subsystem. Then, these fitting functions are used to predict the evaluation results of each subsystem from 2006 to 2020 and calculate the ECC from 2006 to 2020 according to the predicted results. The average percentage error of the ECC from 2006 to 2020 is calculated and shown in Figure 9. It can be seen that the percentage error is very small, and its distribution range is also concentrated at 0–12%, indicating that the overall accuracy of the prediction model is relatively high. Next, the ECC of Yueqing City in 2024 and 2028 is comprehensively calculated using the predicted scores of each subsystem in 2024 and 2028, as shown in Figure 10. From the 2-year forecast results, the spatial characteristics of a few years in the future are basically similar to those of 2006–2020, showing that inland areas are higher than coastal areas, and areas with high population density are higher than areas with low population density. Table 7 lists the ECC evaluation and prediction results of Yueqing City from 2020 to 2028. We can observe from the table that the ECC in Yueqing City has an upward trend, and most areas may reach a better state in 2028.

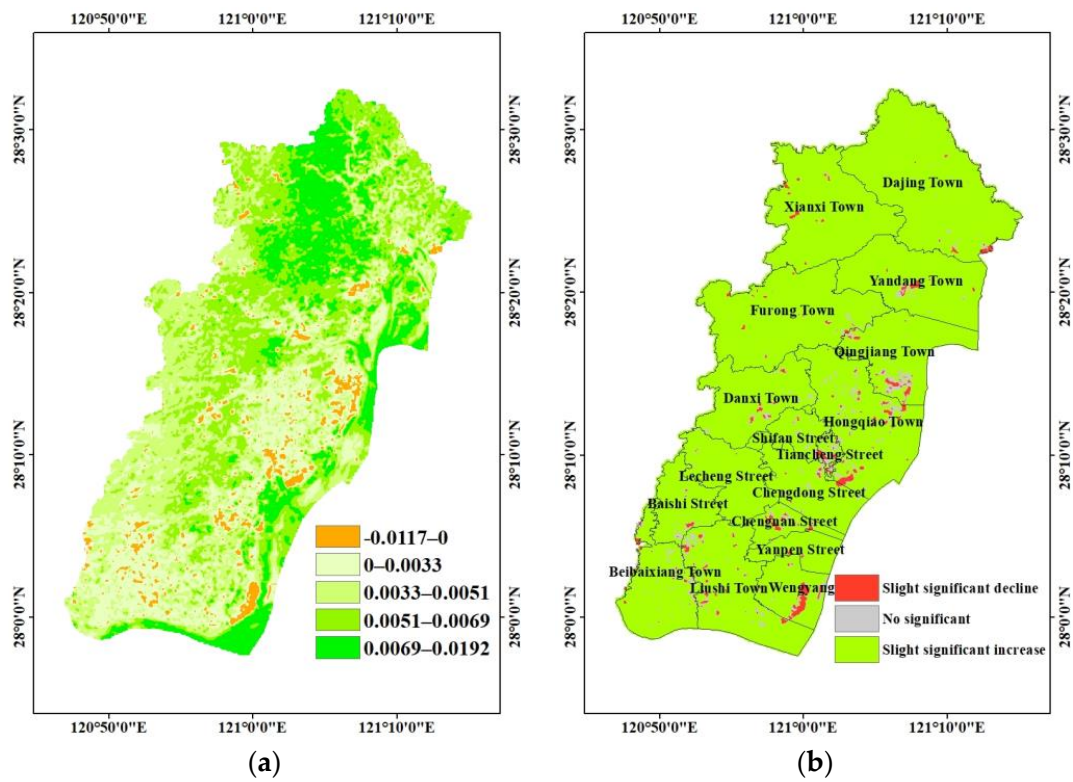


Figure 8. Spatial changes and significant changes of the ECC in Yueqing City. (a) Spatial changes using the Sen's slope estimator. (b) Significant changes using the Mann–Kendall trend test.

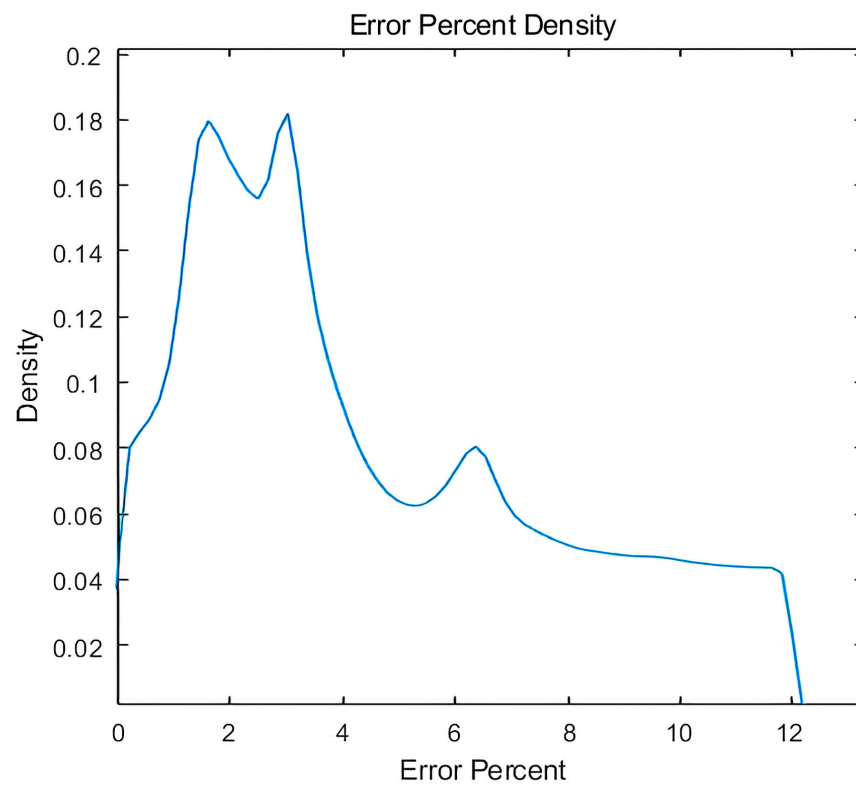


Figure 9. Percent error density plot.

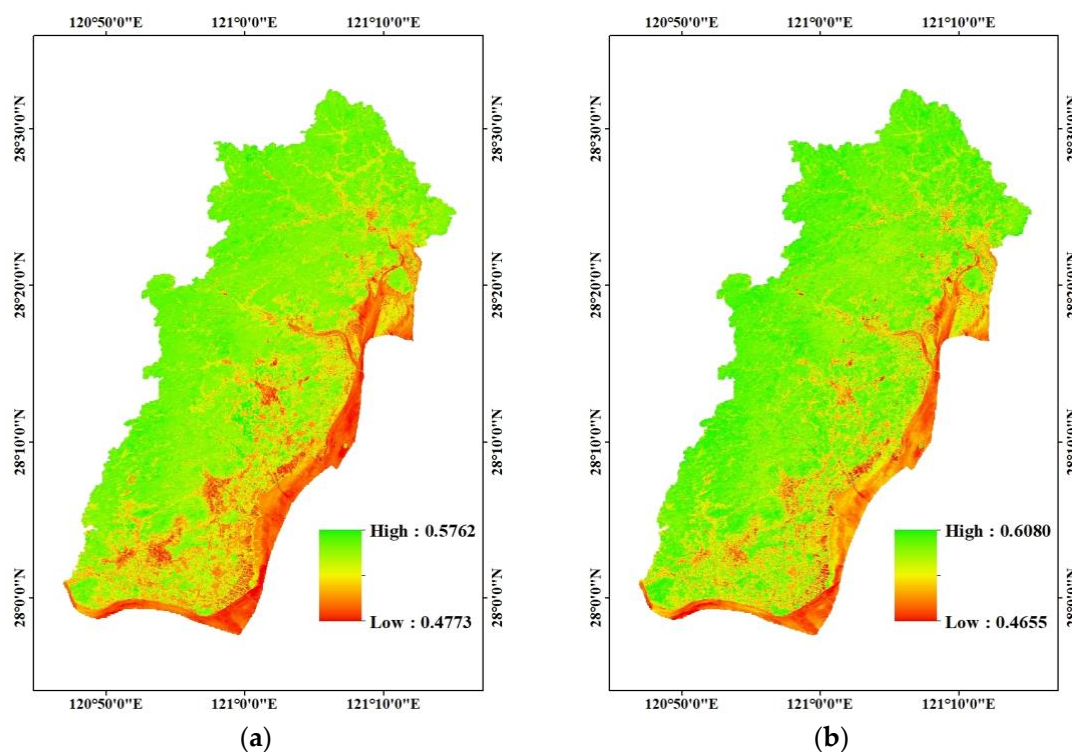


Figure 10. Prediction results of the ECC of Yueqing City in 2024 and 2028. (a) 2024 and (b) 2028.

Table 7. ECC grading prediction results every two years in Yueqing City from 2020 to 2028.

Year	2020	2024	2028
Critical load (0.4–0.45)	13.24%	0	0
Critical load (0.45–0.5)	86.76%	10.11%	1.98%
Critical load (0.5–0.55)	0	47.34%	22.44%
Critical load (0.55–0.6)	0	42.55%	75.58%
Average ECC	0.4728	0.5372	0.5709

In the context of the accelerated urbanization process, Yueqing City’s future planning decisions are also facing great challenges. The above experimental results show that the ECC in Yueqing City showed a recovery growth trend from 2012 to 2018, but there was a significant decline from 2018 to 2020, and it is expected to return to an upward trajectory from 2024 to 2028 years. To address this challenge, a series of measures strengthening environmental protection, monitoring, management, and investment are needed. It is also essential to improve the environmental technologies of relevant industries to reduce emissions. For areas where environmental quality has significantly declined, more effective measures should be taken, such as strengthening law enforcement, establishing reward and punishment mechanisms, and promoting the development of the environmental protection industry. As for areas with severe environmental quality deterioration, more urgent measures are required, including restricting the operation of highly polluting enterprises, temporarily closing heavily polluting factories and enhancing regulatory efforts to rapidly improve environmental quality. In summary, Yueqing City needs to implement various measures to enhance environmental quality to ensure the health and quality of life of its residents.

3.2. Coastline Extraction Results

According to the controlled variable method, the optimal segmentation scale for historical remote sensing images was obtained, as listed in Table 8. Then, the remote sensing image was classified to extract the coastline, and finally, the extracted result was

corrected by combining the remote sensing images. Partial examples of image segmentation results and coastline extraction results are shown in Figures 11 and 12, respectively.

Table 8. Optimal segmentation scales for images at different times.

Year	Segmentation Scale	Shape	Compactness
2006	115	0.8	0.4
2008	120	0.8	0.5
2010	110	0.9	0.5
2012	110	0.8	0.5
2014	100	0.8	0.4
2016	100	0.9	0.4
2018	150	0.7	0.3
2020	160	0.7	0.5

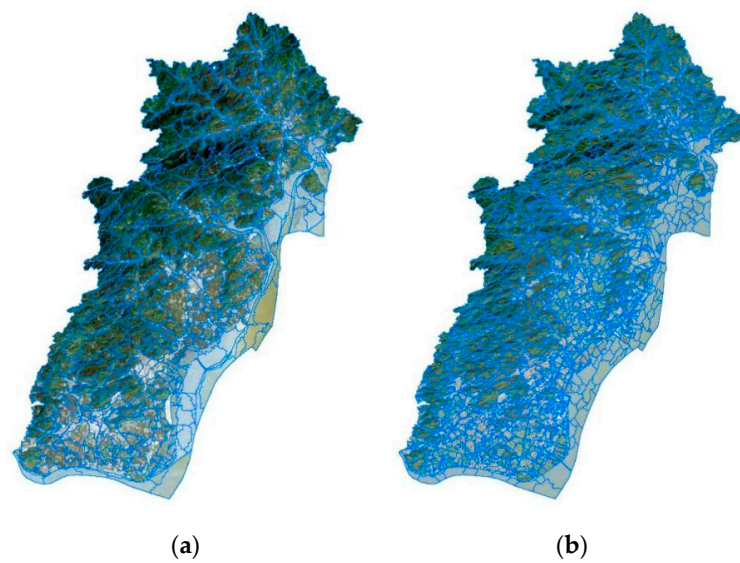


Figure 11. Partial examples of image segmentation results for various years. (a) 2006 and (b) 2020.

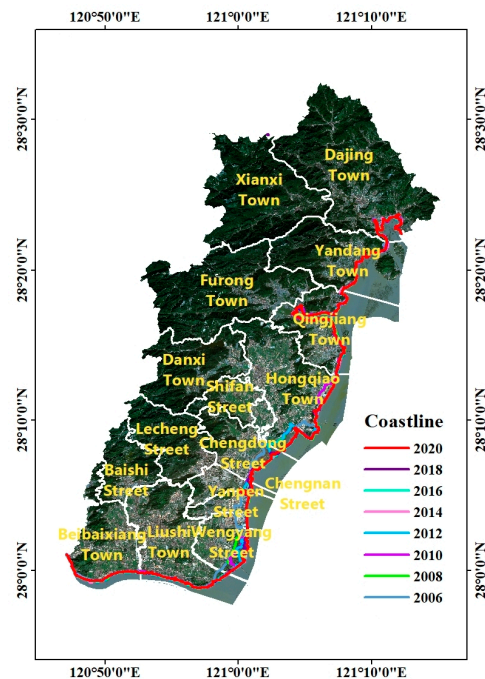


Figure 12. Coastline extraction results at different times.

According to the coastline extraction results, this study calculated the length of the coastline over the years and used ArcGIS 10.7 software to divide the coastline into the natural coastline and artificial coastline according to the coastline interpretation marks. The natural coastline retention rate was calculated by the ratio of the length of the natural coastline to the total length of the coastline. Table 9 lists the coastline length and natural coastline retention rate from 2006 to 2020 with a step size of two years. It can be seen that the length of the coastline has not changed much from 2010 to 2016, but the overall trend has been increasing. Meanwhile, the retention rate of natural coastlines has shown a downward trend. Overall, the length of the natural coastline in 2020 has been shortened by nearly half compared with 2006.

Table 9. Coastline length and natural coastline retention rate at different times.

Year	2006	2008	2010	2012	2014	2016	2018	2020
Coastline length (km)	121.48	123.82	139.41	136.20	137.52	134.69	147.08	156.22
Natural coastline retention rate	20.63%	15.93%	14.72%	12.97%	11.95%	11.55%	8.96%	8.37%

In this study, there are 973 section lines generated based on the DSAS system. The overall distribution of the section lines is shown by the blue markings in Figure 13. According to Figure 14a, it can be observed that the coastline changes of Yueqing City presented an unstable state over the past 15 years, in which the coastlines of Wengyang Street, Yanpeng Street, Chengnan Street, Chengdong Street, and Hongqiao Town have obvious changes, among which the coastline change rate (LRR) around the intersection of No. 230 (Wengyang Street) is as high as 160 m/a. The coastline change rate (LRR) around the intersection of No. 420 (Hongqiao Town) exceeds 100 m/a, and the average coastline change rate around Yanpan Street and Chengnan Street is 50 m/a. The peak value of the coastline change rate in these areas is mainly due to land reclamation, port construction, wharf construction, etc. The detailed analysis is as follows.

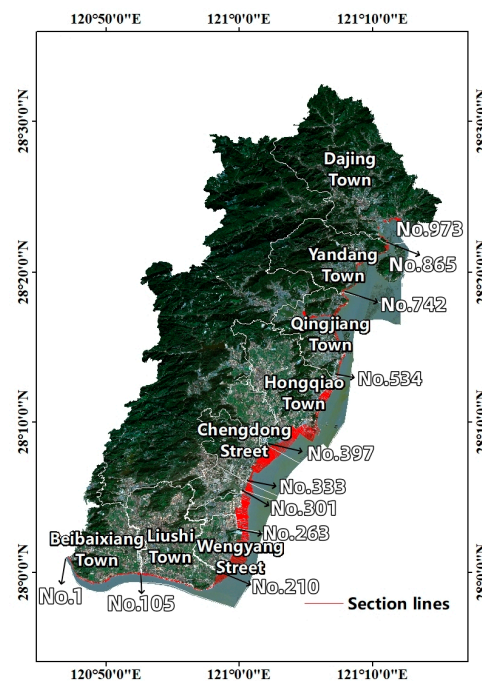


Figure 13. Distribution of section lines.

As shown in Figure 14b, the change in the coastline of Yueqing City over the past 15 years presented a state of first expansion and then stability, in which the change rate was relatively stable from 2008 to 2010, from 2014 to 2016, from 2016 to 2018 and from 2018 to 2020. The average rate in each time period was 106.3 m/a in 2006–2008, 8 m/a in 2008–2010,

23.22 m/a in 2010–2012, 64.9 m/a in 2012–2014, -6.29 m/a in 2014–2016, and -11.1 m/a in 2016–2018. In 2018–2020, it will be 4 m/a. The coastline changes in 2006–2008 and 2012–2014 were more drastic. Yueqing City, relying on good location advantages, has continuously reclaimed land from the sea in Hongqiao Town, Chengdong Street, Chengnan Street, and other areas over the past 15 years and has expanded to the sea. In order to adapt to modern development, the local government established an economic development zone in the coastal area of Yanpan Street and built a port pier in Hongqiao Town. As a result, large-scale land reclamation led to a significant expansion of the coastline. Yueqing City completed a number of ponds during 2008–2013, resulting in a dramatic increase in the coastline in section line number 200–500 from 2006 to 2008, and the maximum rate of coastline change is about 1000 m/a (EPR). From 2010 to 2012, at the 600 intersection (Hongqiao Town), due to the construction of the port, the transition rate was 500 m/a. From 2014 to 2020, because land reclamation projects have basically stopped, the coastline has not changed significantly.

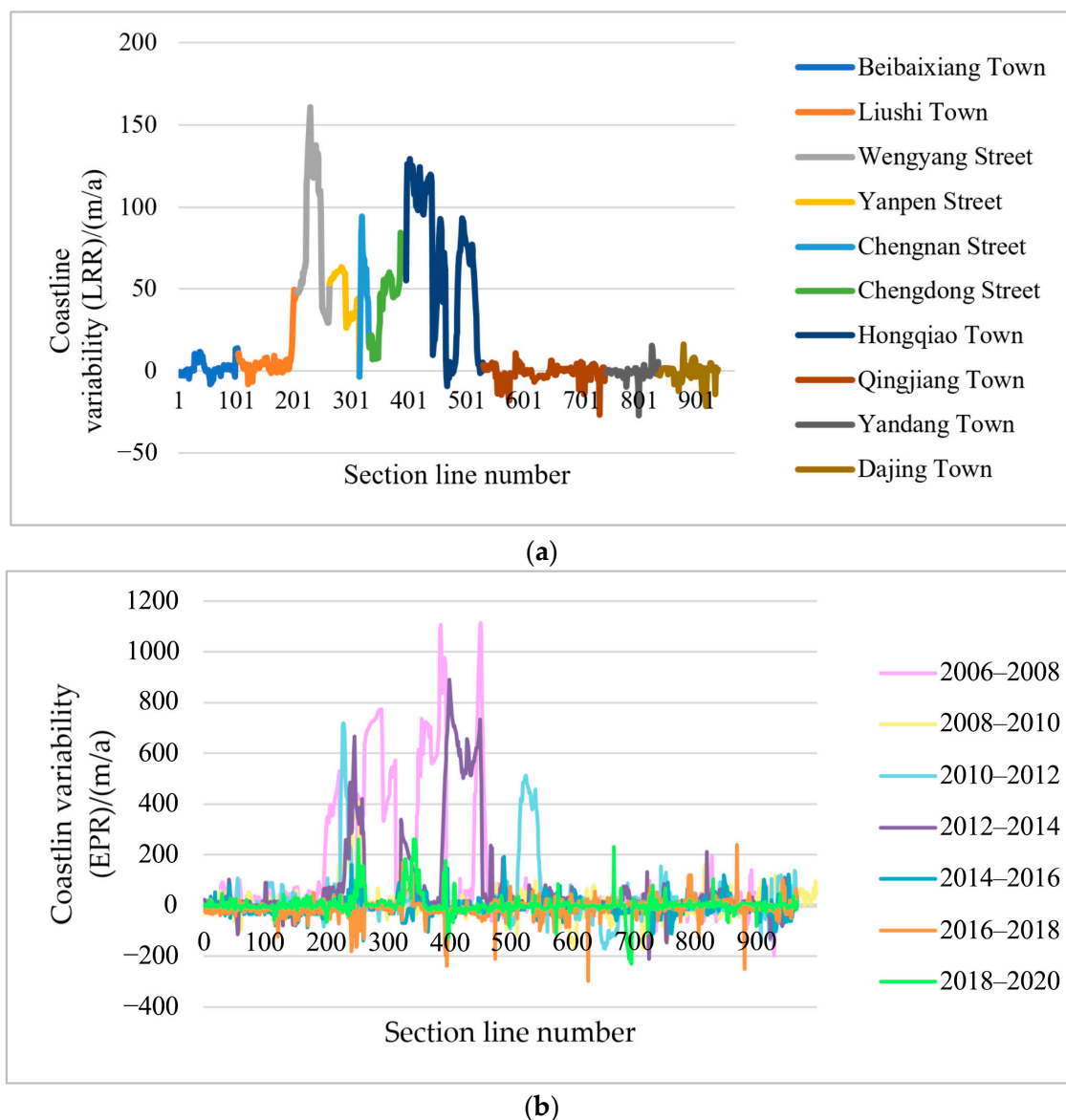


Figure 14. (a) Spatial area variability (LRR) and (b) time variability map (EPR) of Yueqing Coastline.

3.3. Coupling Coordination Degree Analysis of ECC Change and Coastline Transition

We calculated the coupling coordination degree between the annual change rate of ECC and the coastline in Yueqing City, as listed in Table 10.

Table 10. Coupling coordination degree of the ECC changes and coastline changes in Yueqing city.

District	2006–2008	2008–2010	2010–2012	2012–2014	2014–2016	2016–2018	2018–2020
Hongqiao Town	0.289	0.765	0.346	0.957	0.93	0.917	0.425
Liushi Town	0.29	0.763	0.316	0.957	0.932	0.917	0.42
Tiancheng Street	0.29	0.75	0.356	0.957	0.93	0.924	0.408
Dajing Town	0.291	0.758	0.334	0.966	0.922	0.926	0.41
Danxi Town	0.29	0.765	0.051	0.962	0.928	0.924	0.415
Yanpen Street	0.291	0.767	0.208	0.959	0.933	0.906	0.453
Qingjiang Town	0.291	0.763	0.346	0.957	0.931	0.913	0.431
Wengyang Street	0.291	0.765	0.29	0.955	0.933	0.913	0.431
Baishi Street	0.289	0.764	0.265	0.96	0.93	0.922	0.414
Xianxi Town	0.291	0.761	0.27	0.966	0.924	0.925	0.414
Chengnan Street	0.291	0.763	0.255	0.959	0.929	0.915	0.432
Lecheng Street	0.29	0.766	0.29	0.963	0.927	0.922	0.416
Shifan Street	0.291	0.757	0.229	0.962	0.926	0.925	0.419
Furong Town	0.29	0.763	0.27	0.963	0.927	0.922	0.41
Yandang Town	0.292	0.761	0.337	0.963	0.925	0.918	0.429
Beibaixiang Town	0.29	0.762	0.309	0.958	0.929	0.922	0.409
Chengdong Street	0.291	0.768	0.275	0.96	0.93	0.914	0.438
Average	0.29	0.762	0.274	0.96	0.928	0.919	0.422

The coupling coordination degree of the ecological environment and coastline in Yueqing City has gone through several stages of evolution from 2006 to 2020, which is closely related to the change speed of ECC and coastline. During 2006–2008, the ECC declined at a faster rate while the coastline expanded rapidly to the sea. The superposition of these two adverse trends resulted in relatively low coordination between the ECC and coastline change, and the local coupling coordination degree was moderately dysfunctional. During 2008–2010, although the ECC was still declining, the coastline expansion speed slowed down. This trend indicated that the coordination between the ECC and coastline change gradually increased, making the coupling coordination degree upgraded to intermediate coordinated. During 2010–2012, the ECC declined at a faster rate, and the coastline expansion rate also increased. In this case, the two adverse situations echoed each other, decreasing the coupling coordination degree to mildly dysfunctional. During 2012–2018, the ECC maintained positive growth, which meant that the local ecological environment continued to improve. The change rate of the coastline fluctuated and was not obvious. On the whole, the positive change in the ECC had a more significant impact on the coordination degree. During this period, the coupling coordination degree remained at quality coordination. From 2018 to 2020, the ECC continued to decline while the coastline began to expand to the sea. This combination of the deterioration of the ECC and the adverse changes to the coastline resulted in the coupling coordination degree falling to the level of near dysfunctional. Although it has not yet fallen to the level of 2006–2008, great attention should be paid to local ecological and environmental protection.

3.4. Yueqing City Ecological Reconstruction

Figure 8 shows the changing trend of the ECC in Yueqing City over the past 15 years. From the ECC evaluation results, it can be seen that over the past 15 years, the score has declined from 2006 to 2012, recovered from 2012 to 2018, and declined again from 2018 to 2020, and the evaluation results of coastal areas are relatively poor. Among them, the ECC scores of Wengyang Street, Yanpan Street, Chengdong Street, and Hongqiao Town showed a downward trend or a slight upward trend. From the coastline extraction results and the coupling coordination degree between ECC changes and coastline changes, it can

be seen that the coastline has continuously expanded to the sea in the past 15 years, and the changes in the coastline reflect the changing trend of the ECC in the study area to a certain extent. Combined with the above Sen's trend analysis, it can be found that most of the ECC has shown a downward trend in areas where the coastline has changed greatly in the past 15 years. These results indicate that ECC is correlated with coastline changes to a certain extent, and the expansion of coastlines to the sea will reduce wetland area, ecosystem service function, and water exchange capacity, thereby reducing the ECC value. According to the literature review, a number of pond enclosure projects were completed in Yueqing Bay between 2008 and 2013, resulting in the expansion of the coastline and the reduction of tidal wetlands, which also affected water exchange and water quality and led to the decline of the ECC. From 2014 to 2020, the ECC has been restored to a certain extent due to the basic cessation of land reclamation projects, little change in the coastline, and a series of environmental protection measures introduced by Yueqing City.

Based on the above analysis, this study has formulated the following ecological protection and restoration plan tailored to the study area in order to maintain and improve the natural coastline retention rate.

(1) Strict protection of the coastline

The coastlines of Dajing Town, Yandang Town, and Qingjiang Town are located in the north of Yueqing City. The decline in the ECC in this area is small, and the retention rate of the natural coastline is also the highest in the city. However, the coastline in this area has not changed much over the past 15 years and has not advanced to the sea. The overall ecological environment of Yueqing City has deteriorated. The local government should maintain the status quo of the coastline in these areas and prohibit human activities and land reclamation that destroy the topography of the local coastline to effectively guarantee a safe coastline.

(2) Restricted development of the coastline

Beibaixiang Town and Liushi Town are located in the south of Yueqing City. Most of the coastline in these areas is man-made and has a harbor. However, the coastline has not changed much in recent years and has not suffered further damage. Hongqiao Town is located in the middle of Yueqing City, and the coastline of the wharf has changed greatly. For the above-mentioned areas, the local government can retain the existing coastline development activities and no longer carry out projects to change the coastline, such as land reclamation, and properly develop without destroying the coastline environment. In addition, coastline management needs to be strengthened to promote coordination between environmental protection and development.

(3) Renovation and restoration of the coastline

Wengyang Street, Yanpen Street, and Chengdong Street are located in the southeast of Yueqing City. They are the areas where the local coastline has changed the most in the past 15 years, and it is also the area where the ECC has declined the most. In recent years, a large number of human engineering activities, such as land reclamation, have caused the coastline to continue to advance towards the ocean. We should take measures to achieve the goal of a 35% natural coastline retention rate in these areas, including stopping reclamation activities, carrying out coastline restoration work, carrying out ecological construction on the formed artificial coastline, retaining the coastline retreat distance, and speeding up the restoration of ecological functions.

4. Discussion

This paper has proposed an "environment-society-economy-pollution" framework for ECC evaluation, which is more targeted compared to previous generic frameworks such as PSR and DPSIR [16,18]. This study employed a comprehensive weighting method combined with the BPNN to achieve a more precise evaluation of the ECC. Compared to the conventional singular weighting method [55–57], this integrated approach exhibits

greater objectivity and scientific rigor. Upon obtaining the comprehensive evaluation results for the ECC, we utilized the Sen + MK method and incorporated future ECC predictions for analysis, thereby enhancing the accuracy and reliability of the spatiotemporal analysis. It is noteworthy that prior research seldom conducted a comprehensive analysis of the ECC [21,58,59]. Hence, this study delves deeply into the spatial prediction of ECC, providing a more refined spatial analysis tool and decision-making support for environmental protection and sustainable development. Additionally, for the first time, this paper integrates the ECC evaluation of Yueqing City with the results of coastline extraction, thoroughly investigating the correlation between coastline changes and ECC [60]. This offers a novel perspective and strategy for environmental protection and sustainable growth. However, this study still has some shortcomings, which can be improved in future research in the following aspects:

- (1) The choice of evaluation indicators has a direct impact on the evaluation results. While this study considered the characteristics of the research area, data availability, and operability when selecting evaluation indicators, the selection process still possesses a degree of subjectivity due to the multifactorial nature of environmental carrying capacity. Further research is needed to deepen our understanding of indicator selection. Additionally, some important indicators were not included in this study due to data acquisition difficulties. It is hoped that in the future, new methods can be developed to obtain more comprehensive data.
- (2) This study provides predictions for future ECC. However, in order to improve the accuracy and reliability of predictions, sufficient sample support is needed. Due to the limitation of data samples, future research should expand the data volume to enhance the accuracy and reliability of the prediction model.

5. Conclusions

In this study, we proposed an ECC evaluation framework for coastal cities based on the “environment-society-economy-pollution,” especially for the actual situation of Yueqing city. By selecting 18 indicators of the four dimensions of environment, society, economy, and pollution to evaluate the ECC of the research area from 2006 to 2020 and analyzing the changes in the coastline in these years, we calculated and analyzed the coupling coordination degree between ECC changes and coastline changes. In 15 years, Yueqing city’s economy developed rapidly, urbanization level continued to increase, but various pollutants emissions also increased. The total length of Yueqing City’s coastline increased from 121.48 km to 156.22 km, and the natural coastline retention rate decreased from 20.63% to 8.36%. The ECC results showed that the environmental quality experienced the process of deterioration, improvement, and deterioration again. In the future, the ECC is expected to continue to rise, but local ecological environment protection work should not be taken lightly. Based on these findings, we put forward corresponding suggestions for the ecological construction of different regions in the study area.

Author Contributions: Conceptualization, Z.P. and Z.F.; methodology, Z.P.; software, Z.P.; validation, Z.P., Y.W., and Z.F.; formal analysis, Z.P.; investigation, Z.P.; resources, Z.P. and Y.W.; data curation, Z.P.; writing—original draft preparation, Z.P.; writing—review and editing, Z.P. and Y.W.; visualization, Z.P.; supervision, Y.W.; funding acquisition, Y.W. All authors have read and agreed to the published version of the manuscript.

Funding: This work was supported by the Joint Funds of the National Natural Science Foundation of China (U21A2013) and the Key Project of the Open Fund of Key Laboratory of Ocean Space Resource Management Technology (KF-2021-105).

Data Availability Statement: Not applicable.

Conflicts of Interest: The authors declare no conflict of interest.

References

1. Yasir, M.; Sheng, H.; Fan, H.; Nazir, S.; Niang, A.J.; Salauddin, M.; Khan, S. Automatic coastline extraction and changes analysis using remote sensing and GIS technology. *IEEE Access* **2020**, *8*, 180156–180170. [\[CrossRef\]](#)
2. Cisneros, M.A.H.; Sarmiento, N.V.R.; Delrieux, C.A.; Delrieux, C.A.; Piccolo, M.C.; Perillo, G.M. Beach carrying capacity assessment through image processing tools for coastal management. *Ocean Coast. Manag.* **2016**, *130*, 138–147. [\[CrossRef\]](#)
3. Bao, S.; Yang, F. Spatio-Temporal Dynamic of the Land Use/Cover Change and Scenario Simulation in the Southeast Coastal Shelterbelt System Construction Project Region of China. *Sustainability* **2022**, *14*, 8952. [\[CrossRef\]](#)
4. Xu, J.; Li, F.; Suo, A.; Zhao, J.; Su, X. Spatio-temporal Change and Carrying Capacity Evaluation of Human Coastal Utilization in Liaodong Bay, China from 1993 to 2015. *Chin. Geogr. Sci.* **2019**, *29*, 463–473. [\[CrossRef\]](#)
5. Widodo, B.; Lupyanto, R.; Sulistiono, B.; Harjito, D.A.; Hamidin, J.; Hapsari, E.; Yasin, M.; Ellinda, C. Analysis of environmental carrying capacity for the development of sustainable settlement in Yogyakarta urban area. *Procedia Environ. Sci.* **2015**, *28*, 519–527. [\[CrossRef\]](#)
6. Liu, R.; Pu, L.; Zhu, M.; Huang, S.; Jiang, Y. Coastal resource-environmental carrying capacity assessment: A comprehensive and trade-off analysis of the case study in Jiangsu coastal zone, eastern China. *Ocean Coast. Manag.* **2020**, *186*, 105092. [\[CrossRef\]](#)
7. Świąder, M.; Szewrański, S.; Kazak, J.K. Environmental carrying capacity assessment—The policy instrument and tool for sustainable spatial management. *Front. Environ. Sci.* **2020**, *8*, 579838. [\[CrossRef\]](#)
8. Liu, R.Z.; Borthwick, A.G.L. Measurement and assessment of carrying capacity of the environment in Ningbo, China. *J. Environ. Manag.* **2011**, *92*, 2047–2053. [\[CrossRef\]](#)
9. Olgyay, V.; Herdt, J. The application of ecosystems services criteria for green building assessment. *Sol. Energy* **2004**, *77*, 389–398. [\[CrossRef\]](#)
10. Saveriades, A. Establishing the social tourism carrying capacity for the tourist resorts of the east coast of the Republic of Cyprus. *Tour. Manag.* **2000**, *21*, 147–156. [\[CrossRef\]](#)
11. Furuya, K. Environmental carrying capacity in an aquaculture ground of seaweeds and shellfish in Sanriku coast. *Bull. Fish. Res. Agency* **2004**, *1*, 65–69.
12. Cuadra, M.; Björklund, J. Assessment of economic and ecological carrying capacity of agricultural crops in Nicaragua. *Ecol. Indic.* **2007**, *7*, 133–149. [\[CrossRef\]](#)
13. Wu, F.; Zhuang, Z.; Liu, H.L.; Shiau, Y.C. Evaluation of water resources carrying capacity using principal component analysis: An empirical study in Huai'an, Jiangsu, China. *Water* **2021**, *13*, 2587. [\[CrossRef\]](#)
14. Li, X. TOPSIS model with entropy weight for eco geological environmental carrying capacity assessment. *Microprocess. Microsyst.* **2021**, *82*, 103805. [\[CrossRef\]](#)
15. Świąder, M.; Szewrański, S.; Kazak, J.K. Foodshed as an example of preliminary research for conducting environmental carrying capacity analysis. *Sustainability* **2018**, *10*, 882. [\[CrossRef\]](#)
16. Wicaksono, A.P.; Khafid, M.A.; Fakhruddin, F.Z. Evaluation of environment carrying capacity as a coastal tourism using GIS in Sepanjang Beach, Indonesia. *Mater. Sci. Eng.* **2020**, *830*, 032080. [\[CrossRef\]](#)
17. Lane, M. The carrying capacity imperative: Assessing regional carrying capacity methodologies for sustainable land-use planning. *Land Use Policy* **2010**, *27*, 1038–1045. [\[CrossRef\]](#)
18. Zhang, Y.; Fan, J.; Wang, S. Assessment of ecological carrying capacity and ecological security in China's typical eco-engineering areas. *Sustainability* **2020**, *12*, 3923. [\[CrossRef\]](#)
19. Świąder, M.; Lin, D.; Szewrański, S.; Kazak, J.K.; Iha, K.; van Hoof, J.; Belčáková, I.; Altiok, S. The application of ecological footprint and biocapacity for environmental carrying capacity assessment: A new approach for European cities. *Environ. Sci. Policy* **2020**, *105*, 56–74. [\[CrossRef\]](#)
20. Świąder, M.; Szewrański, S.; Kazak, J.K.; Van Hoof, J.; Lin, D.; Wackernagel, M.; Alves, A. Application of ecological footprint accounting as a part of an integrated assessment of environmental carrying capacity: A case study of the footprint of food of a large city. *Resources* **2018**, *7*, 52. [\[CrossRef\]](#)
21. Choi, J.I.; Chung, J.Y.; Hong, G.S. A Study on the Environmental Capacity Assessment in Seoul Metropolitan Area Using Ecological Footprint. *Seoul Stud.* **2011**, *12*, 23–40.
22. Fu, Q.; Jiang, Q.; Wang, Z. Comprehensive evaluation of regional agricultural water and land resources carrying capacity based on DPSIR concept framework and PP model. In *Computer and Computing Technologies in Agriculture V: 5th IFIP TC 5/SIG 5.1 Conference, CCTA 2011, Beijing, China, 29–31 October 2011, Proceedings, Part III 5*; Springer: Berlin/Heidelberg, Germany, 2012; pp. 391–398.
23. Wang, W.; Sun, Y.; Wu, J. Environmental warning system based on the DPSIR model: A practical and concise method for environmental assessment. *Sustainability* **2018**, *10*, 1728. [\[CrossRef\]](#)
24. Maxim, L.; Spangenberg, J.H.; O'Connor, M. An analysis of risks for biodiversity under the DPSIR framework. *Ecol. Econ.* **2009**, *69*, 12–23. [\[CrossRef\]](#)
25. Del Monte-Luna, P.; Brook, B.W.; Zetina-Rejón, M.J.; Cruz-Escalona, V.H. The carrying capacity of ecosystems. *Glob. Ecol. Biogeogr.* **2004**, *13*, 485–495. [\[CrossRef\]](#)
26. Zhang, Y.; Xu, J.; Zeng, G.; Shen, Q.; Hu, Q. The spatial relationship analysis of regional development potential and resource and environment carrying capacity in China. *Geoinformatics* **2008**, *7144*, 714413.

27. Chu, K.; Lu, J. Research on the Coupling Relationship between Marine Resources and Environmental Carrying Capacity and Marine Economy in Jiangsu Province. *Asian J. Econ. Bus. Account.* **2022**, *22*, 1–22.
28. Huang, C.F.; He, L.Z. Model modifications and empirical analysis of the relative carrying capacity of resources. *Resour. Sci.* **2011**, *33*, 41–49.
29. Zhang, Z.; Lu, W.X.; Zhao, Y.; Song, W.B. Development tendency analysis and evaluation of the water ecological carrying capacity in the Siping area of Jilin Province in China based on system dynamics and analytic hierarchy process. *Ecol. Model.* **2014**, *275*, 9–21. [[CrossRef](#)]
30. Li, Y.; Guo, T.; Zhou, J. Research of Ecological Carrying Capacity—Comprehensive Evaluation Model. *Procedia Environ. Sci.* **2011**, *11*, 864–868. [[CrossRef](#)]
31. Wang, L.; Liu, H. Comprehensive evaluation of regional resources and environmental carrying capacity using a PS-DR-DP theoretical model. *J. Geogr. Sci.* **2019**, *29*, 363–376. [[CrossRef](#)]
32. Wang, X.; Wang, S.; Liu, G.; Yan, N.; Yang, Q.; Chen, B.; Bai, J.; Zhang, Y.; Lombardi, G.V. Identification of Priority Areas for Improving Urban Ecological Carrying Capacity: Based on Supply–Demand Matching of Ecosystem Services. *Land* **2022**, *11*, 698. [[CrossRef](#)]
33. Yao, Z.H.; Wang, H.Q.; Hao, X.G. Evaluation of geological environment carrying capacity based on set pair analysis: A case study in Daqing. *Environ. Sci. Technol.* **2010**, *33*, 183–189.
34. Lin, L.; Liu, Y.; Chen, J.N.; Zhang, T.; Zeng, S. Comparative analysis of environmental carrying capacity of the Bohai Sea Rim area in China. *J. Environ. Monit.* **2011**, *13*, 3178–3184. [[CrossRef](#)]
35. Mai, T.; Smith, C. Scenario-based planning for tourism development using system dynamic modelling: A case study of Cat Ba Island, Vietnam. *Tour. Manag.* **2018**, *68*, 336–354. [[CrossRef](#)]
36. Jiang, D.K.; Chen, Z.; Dai, G.L. Evaluation of the carrying capacity of marine industrial parks: A case study in China. *Mar. Policy* **2017**, *77*, 111–119. [[CrossRef](#)]
37. Trang, C.T.T.; Thanh, T.; Thanh, T.D.; Vinh, V.D.; Tu, T.A. Assessment of the environmental carrying capacity of pollutants in Tam Giang-Cau Hai Lagoon (Viet Nam) and solutions for the environment protection of the lagoon. *Sci. Total Environ.* **2021**, *762*, 143130. [[CrossRef](#)]
38. Tan, S.; Liu, Q.; Han, S. Spatial-temporal evolution of coupling relationship between land development intensity and resources environment carrying capacity in China. *J. Environ. Manag.* **2022**, *301*, 113778. [[CrossRef](#)]
39. Feng, Z.; Sun, T.; Yang, Y. The progress of resources and environment carrying capacity: From single-factor carrying capacity research to comprehensive research. *J. Resour. Ecol.* **2018**, *9*, 125–134.
40. Zhang, M.; Liu, Y.; Wu, J.; Yan, H. Index system of urban resource and environment carrying capacity based on ecological civilization. *Environ. Impact Assess. Rev.* **2018**, *68*, 90–97. [[CrossRef](#)]
41. Wang, J.; Sun, T.; Li, P.; Li, F. Research progress on environmental carrying capacity. *J. Appl. Ecol.* **2005**, *16*, 768–772.
42. Zhou, X.Y.; Zheng, B.; Khu, S.T. Validation of the hypothesis on carrying capacity limits using the water environment carrying capacity. *Sci. Total Environ.* **2019**, *665*, 774–784. [[CrossRef](#)]
43. Liao, S.; Wu, Y.; Wong, S.W.; Shen, L. Provincial perspective analysis on the coordination between urbanization growth and resource environment carrying capacity (RECC) in China. *Sci. Total Environ.* **2020**, *730*, 138964. [[CrossRef](#)]
44. Cheng, J.; Zhou, K.; Chen, D.; Fan, J. Evaluation and analysis of provincial differences in resources and environment carrying capacity in China. *Chin. Geogr. Sci.* **2016**, *26*, 539–549. [[CrossRef](#)]
45. Cooper, V.; Molla, A. Information systems absorptive capacity for environmentally driven IS-enabled transformation. *Inf. Syst. J.* **2017**, *27*, 379–425. [[CrossRef](#)]
46. Abbaszadeh Tehrani, N.; Mohd Shafri, H.Z.; Salehi, S.; Chanussot, J.; Janalipour, M. Remotely-Sensed Ecosystem Health Assessment (RSEHA) model for assessing the changes of ecosystem health of Lake Urmia Basin. *Int. J. Image Data Fusion* **2022**, *13*, 180–205. [[CrossRef](#)]
47. Yin, Z.; Li, R.; Li, X.; Meng, H.; Liu, Q.; Yang, N.; Wang, Y.; Tong, X.; Li, C.; Gao, M. Research progress and future development directions of geo-resources and environment carrying capacity. *Geol. China* **2018**, *45*, 1103–1115.
48. Świąder, M. The implementation of the concept of environmental carrying capacity into spatial management of cities: A review. *Manag. Environ. Qual. Int. J.* **2018**, *29*, 1059–1074. [[CrossRef](#)]
49. Wang, S.; Yang, F.L.; Xu, L.; Du, J. Multi-scale analysis of the water resources carrying capacity of the Liaohe Basin based on ecological footprints. *J. Clean. Prod.* **2013**, *53*, 158–166. [[CrossRef](#)]
50. Gilandeh, A.G.; Behjou, F.K.; Yarmohammadi, K. Evaluation of Ardabil City carrying capacity using DPSIR method and ELECTRE model. *Glob. J. Agric. Innov. Res. Dev.* **2018**, *5*, 15–23. [[CrossRef](#)]
51. Cui, D.W. Evaluation and analysis of water resources carrying capacity in Wenshan prefecture based on BP neural network. *J. Yangtze River Sci. Res. Inst.* **2012**, *29*, 9.
52. Li, W.; Xu, G.; Xing, Q.; Lyu, M. Application of improved AHP-BP neural network in CSR performance evaluation model. *Wirel. Pers. Commun.* **2020**, *111*, 2215–2230. [[CrossRef](#)]
53. Hassan, M.F.; Saman, M.Z.M.; Sharif, S.; Omar, B. A Framework for Estimating the Sustainability Index of New Product based on AHP and BP Neural Network. In Proceedings of the 2012 International Conference on Industrial Engineering and Operations Management, Istanbul, Turkey, 3–6 July 2012; pp. 1111–1118.
54. Gens, R. Remote sensing of coastlines: Detection, extraction and monitoring. *Int. J. Remote Sens.* **2010**, *31*, 819–836. [[CrossRef](#)]

55. Yihe, L.V.; Wei, F.U.; Ting, L.I.; Yuanxin, L.I.U. Progress and prospects of research on integrated carrying capacity of regional resources and environment. *Prog. Geogr.* **2018**, *37*, 130–136.
56. Duan, Y.; Mu, H.; Li, N.; Li, L.; Xue, Z. Research on comprehensive evaluation of low carbon economy development level based on AHP-entropy method: A case study of Dalian. *Energy Procedia* **2016**, *104*, 468–474. [[CrossRef](#)]
57. Ye, W.; Xu, X.; Wang, H.; Wang, H.; Yang, H.; Yang, Z. Quantitative assessment of resources and environmental carrying capacity in the northwest temperate continental climate ecotope of China. *Environ. Earth Sci.* **2016**, *75*, 868. [[CrossRef](#)]
58. Naimi-Ait-Aoudia, M.; Berezowska-Azzag, E. Algiers carrying capacity with respect to per capita domestic water use. *Sustain. Cities Soc.* **2014**, *13*, 1–11. [[CrossRef](#)]
59. Ping, Y.X.; Chao, L.E. Early-Warning Model for Tourism Environment Carrying Capacity in Scenic Spots Based on Fuzzy Inference. *Adv. Mater. Res.* **2012**, *373–375*, 605–607.
60. Wang, S.P.; Li, K.Q.; Liang, S.K.; Zhang, P.; Lin, G.; Wang, X. An integrated method for the control factor identification of resources and environmental carrying capacity in coastal zones: A case study in Qingdao, China. *Ocean Coast. Manag.* **2017**, *142*, 90–97. [[CrossRef](#)]

Disclaimer/Publisher’s Note: The statements, opinions and data contained in all publications are solely those of the individual author(s) and contributor(s) and not of MDPI and/or the editor(s). MDPI and/or the editor(s) disclaim responsibility for any injury to people or property resulting from any ideas, methods, instructions or products referred to in the content.